

EVALUATION OF EXISTING MODELS FOR BOND CAPACITY OF NSM FRP

Kourosch NASROLLAHZADEH

*Assistant Professor, Civil Engineering Faculty,
K.N. Toosi University of Technology, Tehran, Iran
nasrollahzadeh@kntu.ac.ir*

Hadi SAMADZAD

*MSc Student, Civil Engineering Faculty, K.N. Toosi University of Technology, Tehran, Iran
hadisamadzad@yahoo.com*

Keywords: Near-Surface Mounted, Bond Strength, CFRP Laminate, Pull-out Test, Bond-Slip Curve

ABSTRACT

It is now nearly two decades since Fiber Reinforced Polymer (FRP) was first used as structural engineering material and ever since its main utilization has been in the strengthening of existing reinforced concrete structures. Flexural and shear strengthening of reinforced concrete elements using FRP are performed in two general methods: externally bonding FRP reinforcement (EBR) to element's surface or putting FRP in the form of rod, laminate and strip in a pre-cut groove and filling it up with epoxy paste. The latter called near-surface mounted FRP (NSM) is more effective method as compared to EBR because higher values of FRP strain can be attained. In order to make an effective use of NSM FRP in strengthening of reinforced concrete structures, it is required to have an adequate understanding of the force transferring mechanism between junction of FRP and concrete. In this paper, three models are implemented and compared with 60 test results using different local bond-slip curves. The first two models are based on fracture mechanics but the second model uses finite element method. The third model is a rather complex closed-form model based on constitutive law and equilibrium. The result of the comparison asserts that the models have accurate predictions for the bond strength of NSM FRP.

INTRODUCTION

The near-surface mounted (NSM) technique is a method to exploit much of the high strength capacity of FRP against another method externally bonded reinforcement (EBR) which is a less efficient method because of lower attainable FRP strain values (De Lorenzis and Teng, 2007). This means that the debonding (loss of bond) failure in EBR method reported in many experimental studies (Sena-Cruz et al., 2012, Teng et al., 2003) can be controlled in the new method.

Utilizing NSM method needs codes and approved instructions based on experimental results and analytical models to determine the strength and the deformation capacity of strengthened RC members and, also, the contribution of FRP in these capacities. Furthermore, in order to develop accurate models for predicting the capacity of flexural or shear strengthened reinforced concrete members, it is required to have an adequate understanding of the force transferring mechanism between junction of FRP and concrete through predictive bond strength models. The homogeneity between analytical models' predictions and experimental results is only one of the essentials that a model must have, also, proposed models must be easy-to-use for engineers in order that they be suitable for applying in codes. Although comprehensive design formulas for EBR technique are provided by ACI-440 committee, studies have been being carried out with the aim of proposing accurate and simple predictive models.

At first, the calculation of the bond capacity of NSM FRP was by assuming a uniform bond stress (τ_b) in the interface of FRP-to-concrete junction (De Lorenzis and Nanni, 2001) but recent studies are predicated on

the fracture mechanic approach and the consideration of a local bond-slip relationship (Seracino et al.2007a). Exploiting this approach through finite element models has led it to make accurate predictions (Zhang et al. 2013a). As regards the simplicity and the accuracy of such models they can be applied in design codes, nonetheless, the mechanical models are more meritorious and have a precedence to numerical models. Bianco et al. (2009) has proposed an accurate predictive model only based on the equilibrium equation and the constitutive law and with considering a multi-linear local bond-slip relationship. In following parts the performance of models proposed by Seracino et al. (2007a), Zhang et al. (2013a) and Bianco et al. (2009) are compared using 60 test specimens extracted from eight experimental programs from the open literature (Zhang et al. 2013a, Bianco et al. 2009).

PROPOSED MODEL BY SERACINO ETAL

Seracino et al. (2007a) proposed a bond strength model using a linear regression analysis with the consideration of the fracture energy and simple linear local bond-slip relationship shown in Fig.1a. The bond strength relation is as described in Eq. (1).

$$P_u = 0.85 \alpha \gamma_g^{0.25} f_c'^{0.33} \sqrt{E_f A_f L_p} \quad (1)$$

where α is equal to 1.0 and 0.85 corresponding to mean value and %95 lower bound of test results, respectively, γ_g is the height to thickness ratio of the pre-cut groove, f_c' (MPa) is the compressive strength of the concrete, L_p (mm) is the perimeter of the fracture according to Eq. (2) (Zhang et al. 2013a), E_f (MPa) and A_f (mm²) are the Young's modulus and the cross section of the FRP strip, respectively.

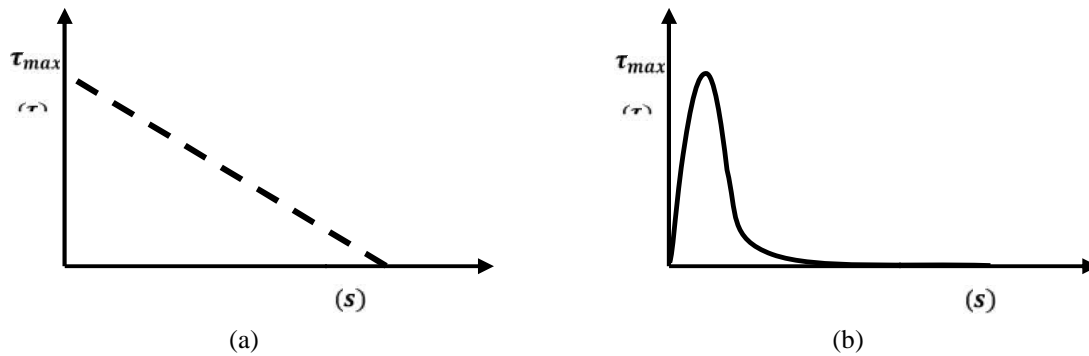


Figure 1. Typical local bond-slip relationships adopted by (a) Seracino et al. (2007a) and (b) Zhang et al. (2013a)

$$L_p = 2 (h_f + 1) + (t_f + 2) \quad (2)$$

where h_f (mm) and t_f (mm) are the FRP strip's height and thickness, respectively. With consideration of parameters such as the effect of the edge distance of the concrete block (β_e) according to Eq. (3) (Rashid et al. 2008), the epoxy paste's cover (c_p) (Oehlers et al. 2008) and the reduction factor of the bond length's shortage (β_L) according to Eq. (4), Zhang et al. (2013a) represented Seracino et al.'s (2007a) model as described in Eq. (5).

$$\beta_e = 0.283 \frac{a_e}{h_f} + 0.196 \leq 1.0 \quad (3)$$

$$\beta_L = \frac{L_b}{L_e} \leq 1.0 \quad (4)$$

$$P_u = 0.85 \alpha \beta_e \beta_L \gamma_g^{0.25} f_c'^{0.33} \sqrt{E_f A_f L_p \left(\frac{h_f + c_p}{c_p} \right)^{1.2}} \quad (5)$$

where in Eq. (3) a_e is the distance of the pre-cut groove to the concrete block's edge and in Eq. (4) L_b and L_e are the embedment length and the effective bond length of the FRP strip according to Eq. (6), respectively.



$$L_e = \frac{\pi}{2(0.802 + 0.078)} \sqrt{\frac{0.976 \gamma_g^{0.526} E_f A_f}{f_c'^{0.6} L_p}} \quad (6)$$

PROPOSED MODEL BY ZHANG ETAL

Zhang et al. (2013a) proposed the bond capacity relation as Eq. (7):

$$P_u = \beta_{L_s} \sqrt{2G_f E_f A_f L_p} \leq P_t \quad (7)$$

where β_{L_s} , G_f (N/mm), E_f (MPa), A_f (mm²), L_p (mm) and P_t are the reduction factor of the bond length's shortage effect, the interfacial fracture energy, the Young's modulus of FRP, the cross section of the strip, the failure perimeter according to Eq. (2) and the ultimate tensile strength of FRP, respectively. G_f is obtained as stated in Eq. (8) from a linear regression analysis on results of a parametric study by implementing a FE model.

$$G_f = 0.40 \gamma_g^{0.422} f_c'^{0.619} \quad (8)$$

In order to considering the effect of the bond length Zhang et al. (2013a) conducted a parametric study on results of a FE model by utilizing the local bond-slip relationship proposed by Zhang et al. (2013b) as a function of γ_g and f_c' which is stated in Eq. (9) and illustrated in Fig. 1b.

$$\tau(s) = A \left(\frac{2B - s}{B} \right)^2 \sin \left(\frac{\pi}{2} \frac{2B - s}{B} \right) \quad s < 2B \quad (9)$$

$$A = 0.72 \gamma_g^{0.138} f_c'^{0.613} \quad (10)$$

$$B = 0.37 \gamma_g^{0.284} f_c'^{0.006} \quad (11)$$

where τ (MPa) and s (mm) are the bond stress and the relative slip between the strip and the concrete, respectively. Providing a closed-form solution when the local bond-slip relationship isn't a simple curve like which is shown in Fig. 1a will be arduous or even implausible, therefore using numerical methods will be inevitable. The maximum value of τ (τ_{max}) is as expressed in Eq. (12) (Zhang et al. 2013a):

$$\tau_{max} = 1.15 \gamma_g^{0.138} f_c'^{0.613} \quad (12)$$

Based on Yuan et al.'s (2004) study, the effective bond length considered by Zhang et al. (2013a) to be equal to the bond length corresponding to a bond strength equal to %99 of the bond strength value in case the infinite embedment length is existent. Furthermore, the governing equation of the junction of FRP and concrete presumed as Eq. (13).

$$\frac{d^2 s}{dx^2} - \frac{2G_f}{\tau_{max}^2} \eta^2 \tau(s) = 0 \quad (13)$$

where η is a constant determinable using Eq. (14).

$$\eta^2 = \frac{\tau_{max}^2 L_p}{2 G_f E_f A_f} \quad (14)$$

The product of the effective bond length (L_e) and η is constant and relies on the ratio between the fracture energy corresponding to the ascending branch and the descending branch of the bond-slip curve (Yuan et al. 2004, Zhang et al. 2013a). Zhang et al. (2013a) obtained the constant value equal to 1.66. Therefore, L_e can be calculated with Eq. (15) and also, the reduction factor of the bond length's shortage

(β_L) is suggested using a curve-fitting to results of the parametric study as stated in Eq. (16).

$$L_e = \frac{1.66}{\eta} \quad (15)$$

$$\beta_L = \frac{L_b}{L_e} \left(2.08 - 1.08 \frac{L_b}{L_e} \right) \quad (16)$$

PROPOSED MODEL BY BIANCO ET AL

The model proposed by Bianco et al. (2009) is a predictive model only based on the equilibrium and the constitutive law. Whereas this mechanical model provides a closed-form solution for the bond capacity of NSM FRP, applying a complex local bond-slip relationship makes the solution hard or even impossible. Bianco et al. (2009) used a multi-linear local bond-slip relationship shown in Fig. 2 by considering four distinct phases as shear load transferring mechanisms. For the sake of the brevity more details are ignored here but are available in Bianco et al. (2009).

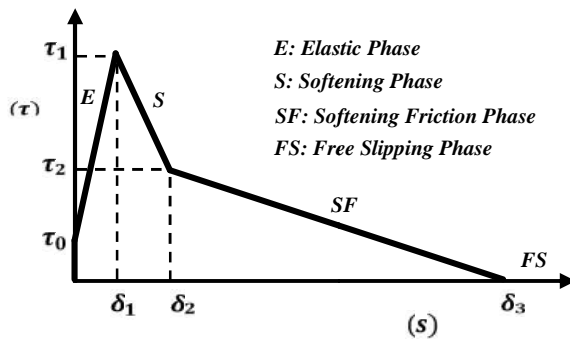


Figure 2. The typical local bond-slip relationship adopted by Bianco et al. (2009).

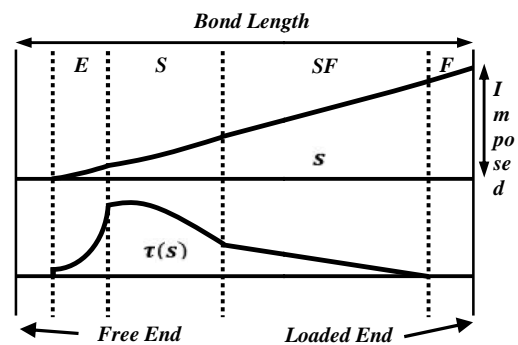


Figure 3. Slip and bond stress distributions along the bond length attained by Bianco et al. (2009).

According to Fig. 2, the governing differential equation obtained from the equilibrium and described in Eq. (17) should be solved for each phase separately by considering the corresponding boundary conditions.

$$\frac{d^2s}{dx^2} - \tau(s) J = 0 \quad (17)$$

where s is the slip of the FRP strip, τ is the bond stress and J is a constant value regarding the ratio of the axial stiffness of FRP and concrete. Firstly, Bianco et al. (2009) achieved the slip distribution along the bond length by solving Eq. (17) for mentioned phases in case the bond length is assumed to be infinite (Fig. 3). As discussed before, the solution is performed for elastic, softening, softening friction and free slipping phases then the boundary conditions imposed separately. The distribution of the bond stress is attainable using the value of the slip in each point along the bond length and according to the local bond-slip relationship shown in Fig. 2. In the next step Bianco et al. (2009) provided the solution for the finite bond length. Thus, by assuming an imposed slip in the loaded end, the caused slip distribution limited to the embedment length. If the bond length is bigger than the required length in which the slip value of the free end is zero, the solution will be as same as the mentioned approach for an infinite bond length. This critical value is the effective bond length discussed in preceding parts. Likewise, when the embedment length is smaller than the effective bond length, slip and stress distribution will be limited according to the imposed end slip and the bond length, consequently, the integration will be performed between these limits. More details are accessible in Bianco et al. (2009).

APPRAISAL OF MODELS

In order to study the performance of discussed models, a comparison performed among the models' accuracy using an experimental database. The database containing 60 pull-out test results on NSM FRP extracted from eight experimental programs, is assembled from the open literature (Zhang et al. 2013a,



Bianco et al. 2009). Characteristics of test specimens and also models' predictive values are listed in Table 1, where L_b is the bond length, h_f and t_f are the width and the thickness of the FRP strip, h_g and w_g are height and width of the pre-cut groove and also b_c and h_c are dimensions of the concrete block. Models' results are also presented in Table 1. Proposed models discussed in the prior parts have been implemented by authors into a computer code. Apart from differences inherent in development of each model, all three models need to presume a bond-slip relationship. As expressed before, the local bond-slip relationship shown in Fig. 1 and stated in Eq. (9) have been used in Seracino et al.'s (2007a) and Zhang et al.'s (2013a), respectively. While, two sets of parameters shown in Fig. 2 have been adopted for the mechanical model of Bianco et al. (2009) (Table 2). The first set is to make the relationship similar to Eq. (9) by determining τ_1 and δ_1 using Eq. (12) and also making another assumptions stated in Table 2. In the second set the value of δ_3 is considered to be equal to 7.12 mm suggested by Bianco et al. (2010) and τ_1 adopted equal to the meanvalue of 60 calculated values in the first set. Furthermore, the value of τ_0 proposed equal to 3.0 MPa with the purpose of considering micromechanical and chemical effects of materials and the interface of the junction (Bianco et al. 2009).

Table 1. Test specimens' characteristics and models' results

*Group	Specimen	Dimensions (mm)						Materials		Test & Models' Result (kN)**									
		L_b	h_f	t_f	h_g	w_g	b_c	h_c	f'_c (MPa)	E_f (GPa)	Test	Z	R	S	R	B1	R	B2	R
1	CS2-30	30	16	4	20	8	150	150	23.2	131	14.8	15.0	1.01	5.2	0.35	8.2	0.55	13.2	0.89
	CS2-100	100	16	4	20	8	150	150	23.2	131	36.3	41.3	1.14	19.3	0.53	26.1	0.72	43.0	1.19
	CS2-150	150	16	4	20	8	150	150	23.2	131	46.1	52.5	1.14	26.0	0.56	34.7	0.75	59.3	1.29
2	DP460NS	152	16	2	19	6.4	202	152	64.5	131	73.4	55.7	0.76	52.8	0.72	45.7	0.62	49.2	0.67
	3M-90-1	305	16	2	19	6.4	458	152	60	131	60.5	54.5	0.90	64.3	1.06	47.8	0.79	66.5	1.10
	3M-90-2	305	16	2	19	6.4	458	152	60	131	62.5	54.5	0.87	64.3	1.03	47.8	0.77	66.5	1.06
	3M-90-3V	305	16	2	19	6.4	458	162	60	131	60.5	54.5	0.90	64.3	1.06	47.8	0.79	66.5	1.10
3	30-Mpa-100-10	100	10	1.2	11	3.2	299	180	30	161.8	22.6	21.8	0.97	12.4	0.55	15.8	0.70	22.5	1.00
	30-Mpa-100-10	100	10	1.22	11	3.2	299	180	30	161.8	20.4	21.9	1.07	12.4	0.61	15.8	0.78	22.5	1.10
	30-MPA-150-10	150	10.3	1.23	11.3	3.2	299	180	30	161.8	23.2	24.3	1.05	19.2	0.83	20.5	0.88	28.8	1.24
	30-MPA-200-10	200	10.5	1.22	11.5	3.2	299	180	30	161.8	27.9	24.5	0.88	26.0	0.93	22.0	0.79	32.7	1.17
	30-Mpa-250-10	250	10.3	1.22	11.3	3.2	299	180	30	161.8	26.6	24.2	0.91	25.9	0.97	22.0	0.83	36.0	1.35
	30-Mpa-300-10	300	10.4	1.22	11.4	3.2	299	180	30	161.8	26.0	24.5	0.94	26.1	1.00	22.7	0.87	39.2	1.51
	30-Mpa-350-10	350	10.4	1.22	11.4	3.2	299	180	30	161.8	23.0	24.5	1.07	26.0	1.13	22.5	0.98	41.2	1.79
	42-Mpa-200-10	200	10.3	1.27	11.3	3.3	299	180	41.8	161.8	30.6	27.4	0.90	29.4	0.96	25.4	0.83	33.5	1.10
	30-Mpa-100-20	100	20	1.2	21	3.2	299	180	30	162.3	51.4	45.2	0.88	27.1	0.53	34.6	0.67	44.2	0.86
	30-Mpa-200-20	200	20	1.2	21	3.2	299	180	30	162.3	57.8	50.6	0.88	54.1	0.94	47.8	0.83	62.4	1.08
	30-Mpa-300-20	300	20	1.2	21	3.2	299	180	30	162.3	66.7	50.6	0.76	55.5	0.83	48.2	0.72	73.8	1.11
	65-Mpa-200-10	200	10.1	2.88	11.1	4.9	301	180	64.8	144.6	45.0	41.3	0.92	39.7	0.88	37.3	0.83	42.1	0.94
	65-Mpa-200-20	200	19.8	2.97	20.8	5	301	180	64.8	162.3	108.8	92.7	0.85	78.1	0.72	74.3	0.68	82.5	0.76
	53-Mpa-200-10	200	10.2	1.24	11.2	3.2	299	180	52.8	161.8	31.9	28.8	0.90	31.2	0.98	26.0	0.82	32.4	1.02
	53-Mpa-200-10	200	10.4	1.3	11.4	3.3	299	180	53	161.8	34.0	30.0	0.88	32.6	0.96	27.6	0.81	33.8	1.00
	53-Mpa-100-20	100	20.2	1.25	21.2	3.3	299	180	53	162.3	63.8	59.1	0.93	39.1	0.61	46.4	0.73	45.8	0.72
	33-Mpa-200-15	200	15.7	1.26	16.7	3.3	299	180	33.4	162.1	47.5	40.5	0.85	42.9	0.90	38.8	0.82	50.3	1.06
	33-Mpa-300-15	300	15.3	1.26	16.3	3.3	299	180	33.4	162.1	51.6	39.3	0.76	42.9	0.83	37.5	0.73	58.4	1.13
	65-Mpa-200-10	200	10	2.9	11	4.9	301	180	64.8	144.6	45.1	41.0	0.91	39.3	0.87	36.8	0.82	41.7	0.93
	33-Mpa-200-20	200	20	1.2	21	3.2	299	180	33.4	162.3	60.7	52.3	0.86	57.5	0.95	49.8	0.82	62.4	1.03

Table 1.(Continued.)

Group*	Specimen	Dimensions (mm)							Materials		Test & Models' Result (kN)**								
		L_b	h_f	t_f	h_g	w_g	b_c	h_c	f'_c (MPa)	E_f (GPa)	Test	Z	R	S	R	B1	R	B2	R
4	12x3	350	12.4	2.76	13.4	4.8	301	180	36.7	146.3	59.2	42.6	0.72	45.3	0.77	40.1	0.68	64.4	1.09
	12x4	350	12.5	4.24	13.5	6.2	300	180	36.7	134.5	54.1	49.5	0.92	52.0	0.96	46.1	0.85	73.3	1.36
	12x6	350	12.4	5.73	13.4	7.7	300	180	36.7	130.5	47.6	54.8	1.15	57.0	1.20	51.2	1.08	81.6	1.71
	24x4	350	24.1	4.33	25.1	6.3	300	180	36.7	141.4	130.0	105.4	0.81	114.0	0.88	101.1	0.78	137.4	1.06
	12x12	350	12	12	13	14	300	180	36.7	131.6	85.9	73.9	0.86	65.0	0.76	69.5	0.81	112.3	1.31
	30x7	350	30.6	7.3	31.6	9.3	299	180	36.7	134.6	165.3	164.9	1.00	141.0	0.85	155.3	0.94	202.6	1.23
	26x20	350	25.3	20.6	26.3	22.6	301	180	36.7	129.8	199.4	198.1	0.99	124.0	0.62	163.2	0.82	258.9	1.30
5	C60NSMa	350	20	1.4	20.8	3	123	180	35.5	161	59.2	57.6	0.97	62.3	1.05	55.4	0.94	82.2	1.39
	C85NSMa	350	20	1.4	20.8	3	173	180	35.5	161	75.7	57.6	0.76	62.3	0.82	55.4	0.73	82.2	1.09
	C150NSMa	350	20	1.4	20.8	3	303	180	35.5	161	63.0	57.6	0.91	62.3	0.99	55.5	0.88	82.3	1.31
	C150NSMb	350	40	2.4	40.8	3	303	180	35.5	173	205.1	175.5	0.86	183.0	0.89	172.1	0.84	196.8	0.96
	G0NSM1	350	20	1.4	20.8	3	297	180	35.5	161	61.2	57.6	0.94	62.3	1.02	55.5	0.91	82.3	1.34
	G0NSM2	350	20	1.4	20.8	3	297	180	35.5	161	64.8	57.6	0.89	62.3	0.96	55.5	0.86	82.3	1.27
6	TS1-3.6-C0	350	10	3.6	11	5.6	300	180	38.8	150	40.0	39.1	0.98	41.1	1.03	36.0	0.90	58.5	1.46
	TS1-3.6-C0R	350	10	3.6	11	5.6	300	180	38.8	160	39.2	40.3	1.03	42.4	1.08	37.2	0.95	59.5	1.52
	TS1-3.6-C10	350	10	3.6	21	5.6	300	180	38.8	165	61.8	61.7	1.00	65.3	1.06	43.4	0.70	60.1	0.97
	TS2-6.0-C0	350	10	6	11	8	300	180	38.8	166	54.8	51.3	0.94	52.2	0.95	47.5	0.87	74.4	1.36
	TS2-6.0-C10	350	10	6	21	8	300	180	38.8	165	86.1	75.7	0.88	80.4	0.93	54.3	0.63	74.3	0.86
	TS2-6.0-C20	350	10	6	31	8	300	180	38.8	169	136.0	98.4	0.72	104.0	0.77	58.5	0.43	74.8	0.55
	TS3-6.0-C15	350	10	6	26	8	300	180	38.8	160	89.8	85.4	0.95	90.5	1.01	55.3	0.62	73.6	0.82
	TS3-6.0-C25	350	10	6	36	8	300	180	38.8	161	117.0	106.0	0.91	111.0	0.95	59.8	0.51	73.7	0.63
	TS3-6.0-C30	350	10	6	41	8	300	180	38.8	160	129.9	115.2	0.89	120.0	0.92	61.1	0.47	73.6	0.57
	TS3-6.0-C40	350	10	6	51	8	300	180	38.8	154	130.6	130.8	1.00	135.0	1.03	62.8	0.48	72.6	0.56
7	7-R-60-S-6.4	230	16	2	20	6	110	220	71.1	151	50.8	64.3	1.27	72.5	1.43	55.4	1.09	61.3	1.21
8	fcm35_Lb40	40	9.34	1.39	15	3.3	100	180	35	158.3	15.0	17.3	1.15	-	-	8.4	0.56	10.1	0.67
	fcm45_Lb40	40	9.34	1.39	15	3.3	100	180	45	158.3	15.5	19.9	1.28	-	-	9.8	0.63	10.1	0.65
	fcm70_Lb40	40	9.34	1.39	15	3.3	100	180	70	158.3	15.7	25.3	1.61	-	-	13.3	0.85	10.1	0.64
	fcm35_Lb60	60	9.34	1.39	15	3.3	100	180	35	158.3	22.8	23.3	1.02	-	-	12.0	0.53	14.2	0.62
	fcm45_Lb60	60	9.34	1.39	15	3.3	100	180	45	158.3	19.9	23.3	1.17	-	-	14.1	0.71	14.2	0.71
	fcm70_Lb60	60	9.34	1.39	15	3.3	100	180	70	158.3	18.9	32.8	1.74	-	-	17.4	0.92	14.2	0.75
	fcm35_Lb80	80	9.34	1.39	15	3.3	100	180	35	158.3	22.4	27.6	1.23	-	-	14.8	0.66	18.5	0.83
	fcm45_Lb80	80	9.34	1.39	15	3.3	100	180	45	158.3	26.4	30.8	1.17	-	-	16.7	0.63	18.5	0.70
fcm70_Lb80	80	9.34	1.39	15	3.3	100	180	70	158.3	25.6	37.0	1.45	-	-	20.8	0.81	18.6	0.73	

* Groups 1 to 8 are extracted from Li et al. (2005), Shield et al. (2005), Seracino et al. (2007b), Seracino et al. (2007a), Rashid et al. (2008), Oehlers et al. (2008), Perera et al. (2009) and Sena-Cruz and Barros (2004), respectively.

** Z: Zhang et al. (2013a), S: Seracino et al. (2007a), B: Bianco et al. (2009), R: Ratio

Table 2. Parameter sets adopted in Bianco et al.'s (2009) model.

Set	Bond Stress Parameters (MPa)			Slip Parameters (mm)		
	τ_0	τ_1	τ_2	δ_1	δ_2	δ_3
1	3.00	Eq. (12)	0.10	Eq. (9)	$0.9\delta_3$	$2B$ (Eq. 11)
2	3.00	13.40	$4.02(0.3\tau_1)$	0.10	1.00	7.12

Results of the comparison are listed in Table 1. Moreover, Figures 4a and 4b show comparison of the predicted values of three mentioned models against test results for bond strength values in range of 0-60kN and 60-260kN, respectively.



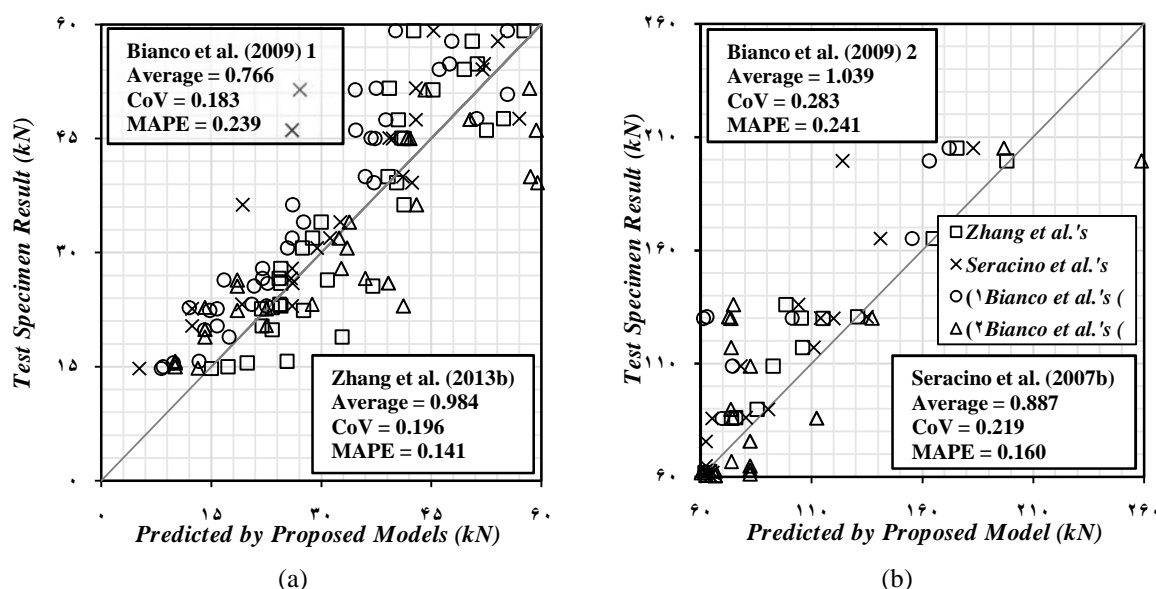


Figure 4. Comparison of the models' predicted bond strengths against test result collection (a) in range of 0-60 kN and (b) in range of 60-260 kN

CONCLUSIONS

In this paper the performance of three models proposed by Seracino et al. (2007a), Zhang et al. (2013a) and of Bianco et al. (2009) has been studied using experimental results. The first two models were based on fracture mechanics and the third model has been predicated on the equilibrium and the constitutive law and executed by adopting two sets of local bond-slip parameters suggested by authors.

Statistical parameters corresponding to mentioned models' outputs give that these models have accurate predictions for the bond strength of NSM FRP. The coefficient of variation (CoV) of the mechanical model with parameter set 1 is minimum among other two models but the model proposed by Zhang et al. (2013a) has the maximum value of the average and the minimum value of the mean absolute percentage error. The suggested parameter set for the mechanical model with the aim of providing a unique local bond-slip relationship has improved the accuracy of the model as regards average and the same CoV values against the resulted value obtained using parameter set 1 as demonstrated in Fig. 4.

Although the mechanical model has a desirable accuracy with the purpose of applying it in design codes, further studies should be carried out to simplify it by considering the effectiveness of its parameters and procedures.

REFERENCES

- ACI Committee 440 (2008) *Guide for the design and construction of externally bonded FRP systems for strengthening concrete structures*, American Concrete Institute
- Bianco V, Barros J A and Monti G (2009) Bond model of NSM-FRP strips in the context of the shear strengthening of RC beams, *Journal of Structural Engineering*, 135(6): 619-631
- Bianco V, Monti G and Barros JAO (2010) Theoretical model and computational procedure to evaluate the NSM FRP strips shear strength contribution to a RC beam, *Journal of Structural Engineering*, 137(11): 1359-1372
- De Lorenzis L and Nanni A (2001) Shear strengthening of reinforced concrete beams with near-surface mounted fiber-reinforced polymer rods, *ACI Structural Journal*, 98(1)
- De Lorenzis L and Teng JG (2007) Near-surface mounted FRP reinforcement: An emerging technique for strengthening structures, *Journal of Composites Part B: Engineering*, 38(2): 119-143
- Li R, Teng JG and Yue QR (2005) Experimental study on bond behavior of NSM CFRP strips-concrete interface, *Ind Constr*, 35(8): 31-35

- Oehlers DJ, Haskett M, Wu C and Seracino R (2008) Embedding NSM FRP plates for improved IC debonding resistance, *Journal of Composites for Construction*, 12(6): 635-642
- Perera WKK G, Ibell TJ and Darby A P (2009, July) Bond behavior and effectiveness of various shapes of NSM CFRP bars, In *Proc of the 9th international symposium on fiber-reinforced polymers reinforcement for concrete structures (FRPRCS-9)*, Sidney, Australia: 13-15
- Rashid R, Oehlers DJ and Seracino R (2008) IC debonding of FRP NSM and EB retrofitted concrete: Plate and cover interaction tests, *Journal of Composites for Construction*, 12(2): 160-167
- Sena-Cruz JM and Oliveira de Barros JA (2004) Bond between near-surface mounted carbon-fiber-reinforced polymer laminate strips and concrete, *Journal of composites for construction*, 8(6): 519-527
- Sena-Cruz José M, Barros Joaquim AO, Mário RF Coelho and Luís FFT Silva (2012) Efficiency of different techniques in flexural strengthening of RC beams under monotonic and fatigue loading, *Journal of Construction and Building Materials*, 29: 175-182
- Seracino R, Jones NM, Ali MSM, Page MW and Oehlers DJ (2007a) Bond strength of near-surface mounted FRP strip-to-concrete joints, *Journal of Composites for Construction, ASCE*, 11(4): 401-409
- Seracino R, RaizalSaifulnaz MR and Oehlers DJ (2007b) Generic debonding resistance of EB and NSM plate-to-concrete joints, *Journal of Composites for Construction*, 11(1): 62-70
- Shield C, French C and Milde E (2005) the effect of adhesive type on the bond of NSM tape to concrete, *ACI Special Publication*, 230
- Teng JG, Smith ST, Yao J and Chen JF (2003) Intermediate crack-induced debonding in RC beams and slabs, *Construction and building materials*, 17(6): 447-462
- Yuan H, Teng JG, Seracino R, Wu ZS and Yao J (2004) Full-range behavior of FRP-to-concrete bonded joints, *Engineering Structures*, 26(5): 553-565
- Zhang SS, Teng JG and Yu T (2013a) Bond Strength Model for CFRP Strips Near-surface Mounted to Concrete, *Journal of Composites for Construction, ASCE*, 18(3)
- Zhang SS, Teng JG and Yu T (2013b) Bond-slip model for CFRP strips near-surface mounted to concrete, *Engineering structures*, 56: 945-953

